© 2014. Published by The Company of Biologists Ltd | Development (2014) 141, 2813-2824 doi:10.1242/dev.107276

RESEARCH ARTICLE

Initiation of Hippo signaling is linked to polarity rather than to cell position in the pre-implantation mouse embryo

Shihadeh Anani[1,2], Shivani Bhat[1], Nobuko Honma-Yamanaka[1], Dayana Krawchuk[1] and Yojiro Yamanaka[1,2,*]

ABSTRACT

In the mouse embryo, asymmetric divisions during the 8-16 cell division generate two cell types, polar and apolar cells, that are allocated to outer and inner positions, respectively. This outer/inner configuration is the first sign of the formation of the first two cell lineages: trophectoderm (TE) and inner cell mass (ICM). Outer polar cells become TE and give rise to the placenta, whereas inner apolar cells become ICM and give rise to the embryo proper and yolk sac. Here, we analyze the frequency of asymmetric divisions during the 8-16 cell division and assess the relationships between cell polarity, cell and nuclear position, and Hippo signaling activation, the pathway that initiates lineage-specific gene expression in 16-cell embryos. Although the frequency of asymmetric divisions varied in each embryo, we found that more than six blastomeres divided asymmetrically in most embryos. Interestingly, many apolar cells in 16-cell embryos were located at outer positions, whereas only one or two apolar cells were located at inner positions. Live imaging analysis showed that outer apolar cells were eventually internalized by surrounding polar cells. Using isolated 8-cell blastomeres, we carefully analyzed the internalization process of apolar cells and found indications of higher cortical tension in apolar cells than in polar cells. Last, we found that apolar cells activate Hippo signaling prior to taking inner positions. Our results suggest that polar and apolar cells have intrinsic differences that establish outer/inner configuration and differentially regulate Hippo signaling to activate lineage-specific gene expression programs.

KEY WORDS: YAP (Yes-associated protein), Asymmetric division, Cell sorting, 16-cell stage, Inner cell mass (ICM), Trophectoderm (TE), Live imaging, Mouse

INTRODUCTION

Three divisions after fertilization, the 8-cell mouse embryo initiates two morphogenetic processes: compaction and polarization (Saiz and Plusa, 2013; Yamanaka et al., 2006). Compaction minimizes embryo surface area and polarization establishes apico-basal cell polarity in each blastomere. After the 8-cell stage, distinct outer and inner cell populations arise, indicating the formation of the first two embryonic cell lineages: trophectoderm (TE) and inner cell mass (ICM). It is widely accepted that asymmetrical division of 8-cell blastomeres during the 8-16 cell division is crucial for formation of inner cells. Pioneering work by Johnson and Ziomek suggested that the apical pole of a polarized 8-cell blastomere is often asymmetrically inherited after 8-16 cell divisions to generate two cell populations: polar and apolar daughter cells (Johnson and Ziomek, 1981). Apolar cells take an inner position to form the ICM of the blastocyst, giving rise to the fetus and yolk sac, whereas polar cells take outer positions to form the TE, giving rise to the placenta. Establishment of outer/inner cell position after the 16-cell stage is important to restrict expression of lineage-specific transcription factors in order to promote position-specific cell fates, although these cells still retain lineage plasticity (Suwinska et al., 2008).

It is still unknown what controls the symmetrical or asymmetrical division of an 8-cell blastomere but it is known that the frequency of asymmetric divisions varies from one embryo to another. Several studies have measured the number of outer/inner cells in the 16-cell stage embryo using various methods (Dietrich and Hiiragi, 2007; Fleming, 1987; McDole et al., 2011; Morris et al., 2010; Suwinska et al., 2008; Yamanaka et al., 2010). In studies using a combination of outer cell labeling and cell dissociation, the number of inner cells scored tends to be high, whereas in studies measuring nuclear position with confocal microscopy on intact embryos, the number of inner cells scored tends to be low. Although asymmetric division is originally defined as asymmetric inheritance of an apical domain, there are no studies that directly examine the relationship between the number of outer/inner cells and the number of polar/apolar cells in the intact 16-cell embryo. In addition, it is not fully known how outer/inner cells are established in the 16-cell embryo. One possibility is that positioning of outer/inner cells is due to the direction of division orientations during the 8-16 cell divisions. When the mitotic spindle is perpendicular to the embryo surface, one daughter cell is embedded in an inner position and the other is left in an outer position. When it is parallel, both daughter cells are left in outer positions. However, previous live-imaging studies (McDole et al., 2011; Sutherland et al., 1990; Yamanaka et al., 2010) showed that division orientations of most dividing 8-cell blastomeres are oblique instead of perpendicular or parallel to the embryo surface. Additionally, both daughter cells might be placed at an outer position soon after division but often one daughter cell is internalized (Yamanaka et al., 2010; McDole et al., 2011). This suggests that a cell sorting process is also involved in setting up the outer/inner configuration in the 16-cell embryo.

At the molecular level, the transcription factor CDX2 is specifically expressed in the TE (derived from outer cells) and is essential for TE formation (Blij et al., 2012; Ralston and Rossant, 2008; Strumpf et al., 2005; Wu et al., 2010). The Hippo/YAP signaling cascade has been shown to control TE-specific CDX2 expression (Cockburn et al., 2013; Hirate et al., 2013; Leung and Zernicka-Goetz, 2013; Nishioka et al., 2009; Sasaki, 2010). YAP is a transcriptional co-activator that is shuttled between the nucleus and the cytoplasm in a phosphorylation-dependent manner. As early as the 16-cell stage, YAP nuclear localization is observed in outer cells where it will bind TEAD4 and activate *Cdx2* expression. At the same time, cytoplasmic phosphorylated YAP (p-YAP) is observed in inner cells excluded from the nucleus. It has been shown that YAP regulation is necessary and sufficient for TE lineage

[1]Goodman Cancer Research Centre, McGill University, 1160 Pine Avenue West, Montreal, QC H3A1A3, Canada. [2]Department of Human Genetics, McGill University, 1160 Pine Avenue West, Montreal, QC H3A1A3, Canada.

*Author for correspondence (yojiro.yamanaka@mcgill.ca)

Received 18 December 2013; Accepted 15 May 2014

Development (2014) 141, 2813-2824 doi:10.1242/dev.107276

specification (Nishioka et al., 2009). Interestingly, experimental manipulations of YAP signaling can alter lineage-specific gene expression in the embryo, but cannot affect establishment of outer/inner cells, suggesting that the YAP signaling cascade functions downstream of cell position.

Here, we carefully analyzed the number of polar/apolar cells and outer/inner cells in intact 16-cell embryos. We found that many apolar cells were located in an outer position at the 16-cell stage with only one or two cells fully internalized. Live imaging analysis confirmed the presence of outer apolar cells and showed their internalization process. Notably, many of these outer apolar cells had high cytoplasmic p-YAP, an early marker for inner cells, suggesting that differential YAP regulation is initiated by a difference in cell polarity, rather than cell position. Analysis of isolated 8-cell blastomeres confirmed that polar and apolar cells had intrinsic differences in the regulation of p-YAP soon after division and before setting up outer/inner configurations in the embryo.

RESULTS

Variability in asymmetric division frequency during the 8-16 cell division

To directly analyze the number of polar/apolar cells in the intact embryo and correlate it to outer/inner position in the embryo, we counted the number and scored the position of polar and apolar cells in intact 16-cell embryos. To identify polar cells, we visualized apical domains using phospho-ezrin/radixin/moesin (p-ERM) antibody staining. ERM family proteins function as linkers between cell membrane proteins and the F-actin cytoskeleton (Fehon et al., 2010). Ezrin is localized to apical microvilli of epithelial cells and polarized early mouse blastomeres (Berryman et al., 1993; Dard et al., 2001; Louvet et al., 1996). In contrast to apical domain markers such as PARD6B, p-ERM is restricted to the apical domain and is not localized basolaterally (Fig. 1A,E). Prominent p-ERM staining was observed at the 8-cell stage as a ring/cap on each blastomere and co-localized with enrichment of F-actin and PARD6B (Fig. 1A,D,E). At the 16-cell stage, each apical domain was still clearly visible, despite starting to interconnect and encompass the surface of the embryo (Fig. 1B,C).

To analyze how many polar/apolar cells were in 16-cell mouse embryos, we collected freshly flushed CD1 embryos at the 16-cell stage (Fig. 2A) as well as cultured CD1 embryos from the 8-cell stage to 16-cell stage (Fig. 2B). As previously reported (Table 1), we observed variability in the number of polar cells from 8 to 14 polar cells/embryo (n=20) in freshly flushed embryos (Fig. 2A). In our hands, 75% of the embryos had 8-10 polar cells. We observed similar results in cultured CD1 embryos from the 8-cell stage (Fig. 2B, n=26, mean polar cell number is 10.4±0.38 cells/embryo). When we analyzed B6 embryos to examine whether mouse strain identity affected the number of polar cells at the 16-cell stage, we observed a higher average number of polar cells in cultured B6 embryos but not in flushed B6 embryos (Fig. 2C,D, 10.5±0.28 cells/flushed B6 embryo, 11.7±0.38 cells/cultured B6 embryo). Although there is similar variability in the number of polar cells (a range of 8 to 15 cells) and no difference between flushed CD1 and flushed B6 embryos, the distribution pattern of polar cell numbers in cultured B6 embryos is significantly different from others (Mann-Whitney U-test, P<0.05 between CD1 and B6 cultured embryos and between B6 flushed and cultured). This indicated that cultured B6 embryos tended to have more polar cells at the 16-cell stage.

To use the number of polar/apolar cells for estimating the frequency of asymmetric divisions of 8-cell blastomeres, we examined apical domain dynamics during and after division. Immunostaining analysis of fixed embryos showed that both PARD6B and p-ERM maintained their apical localization through the mitotic phase (Fig. 1D,E; supplementary material Fig. S1). Live imaging analysis using apical domain reporters such as Ezrin-GFP/RFP and membrane-RFP, also confirmed the inheritance of the apical domain from parental 8-cell blastomeres (supplementary material Fig. S2). Although repolarization of inner cells after immunosurgery has been reported (Hogan and Tilly, 1978; Spindle, 1978; Stephenson et al., 2010), repolarization of apolar cells in intact 16-cell embryos was a rare event (supplementary material

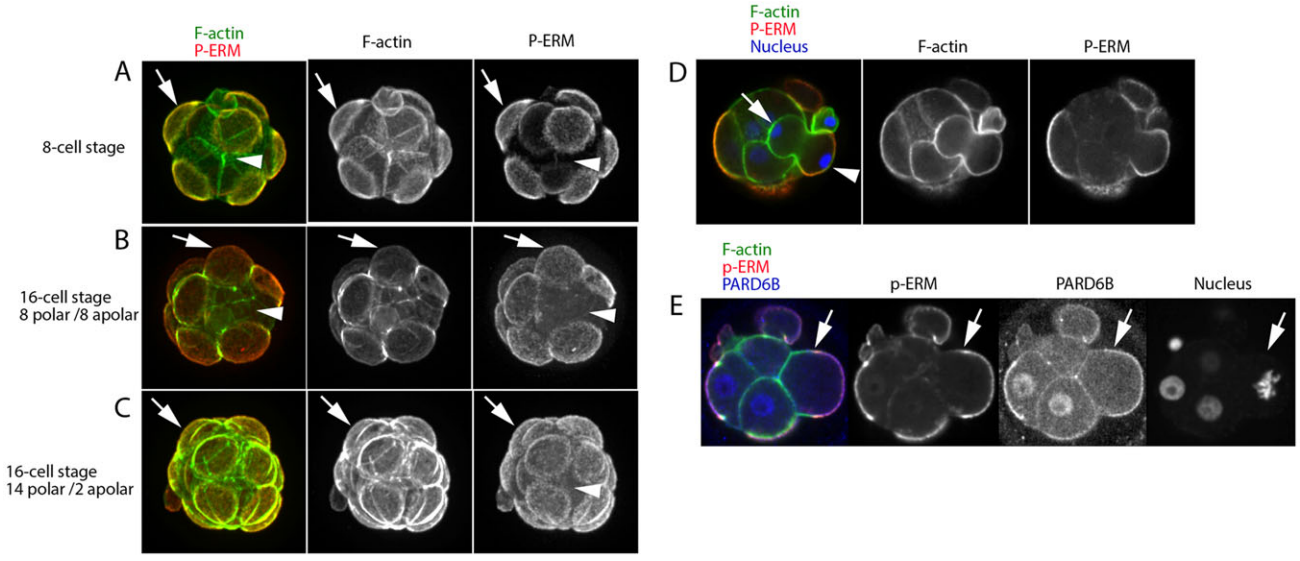

Fig. 1. Inheritance of the apical domain through 8-16 cell divisions. (A) Eight-cell polarized embryo. Projected images. Apical domains (arrows) are prominent ring/cap-like stainings of F-actin and p-ERM. (B) Sixteen-cell embryo with eight polar and eight apolar cells. (C) 16-cell embryo with 14 polar and two apolar cells. At the 16-cell stage, none of the embryos were fully encompassed by apical domains. Surfaces with no apical domains (arrowhead). (D,E) Apical domains were maintained during the 8-cell division. Confocal optical section images. More examples are shown in supplementary material Fig. S1. (D) p-ERM labeled apical domain was maintained during asymmetric 8-cell division. Arrow and arrowhead indicate forming apolar and polar daughter cells, respectively. (E) Apical PARD6B enrichment (arrows) was maintained during 8-cell division.

Development (2014) 141, 2813-2824 doi:10.1242/dev.107276

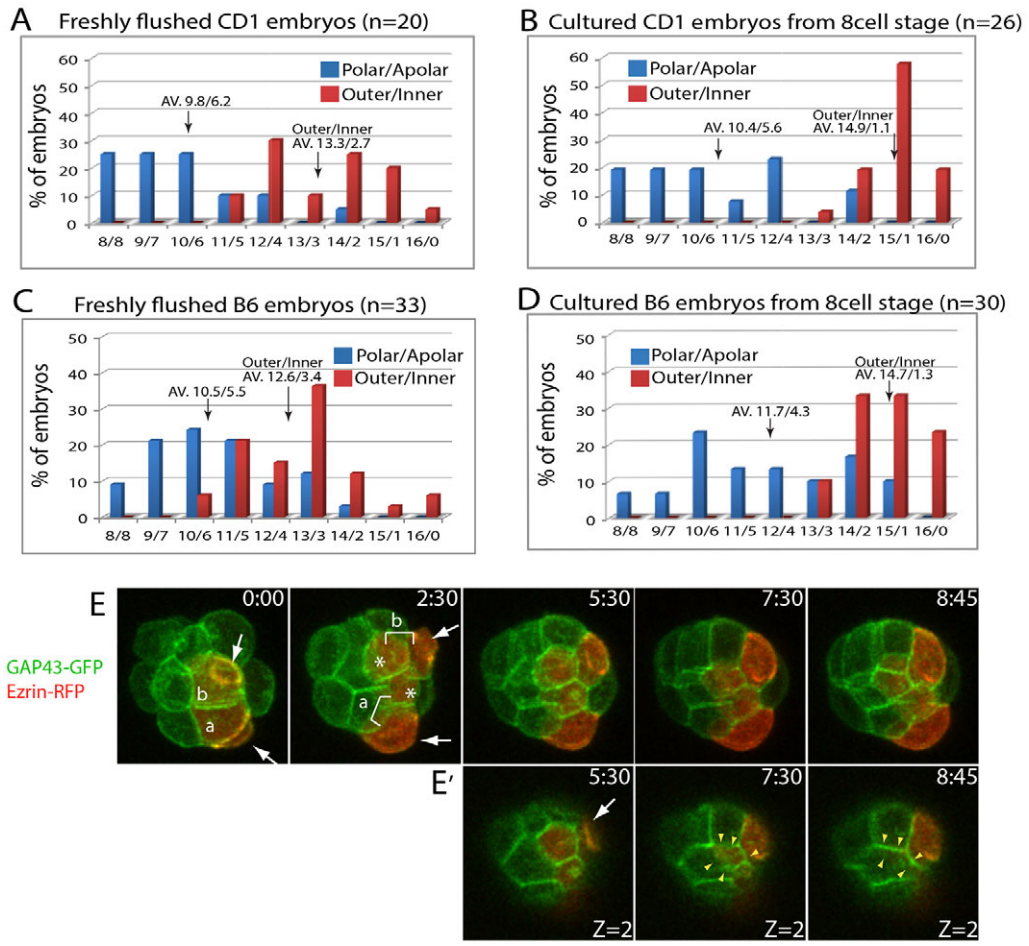

Fig. 2 . Outer apolar cells in 16-cell embryos and their internalization process. (A) The number of polar/apolar and outer/inner cells in freshly flushed CD1 16-cell embryos (*n*=20). (B) Cultured CD1 16-cell embryos (*n*=26). (C) Freshly flushed B6 16-cell embryos (*n*=33). (D) Cultured B6 16-cell embryos (*n*=30). A significant difference was observed between flushed and cultured B6 embryos and between cultured CD1 and cultured B6 embryos (Mann-Whitney U-test, $P<0.05$) but not between flushed CD1 and B6 or between flushed and cultured CD1 embryos. The average numbers of polar/apolar cells and outer/inner cells are shown in each graph. (E,E′) Time-lapse images of internalizing apolar 16 cells. An embryo labeled with GAP43-GFP and Ezrin-RFP. Ezrin-RFP mRNA was injected into one cell of a four-cell embryo. (E) Projected images. (E′) Optical section (Z=2/9). (t=0:00) Two eight-cell blastomeres (a,b) labeled with Ezrin-RFP enriched at apical domains (arrows). (t=2:30) Both 8-cell blastomeres divided asymmetrically. Sister pairs are marked with brackets. Apolar cells are marked with asterisks. The time of cytokinesis of blastomeres a and b are t=1:15 and t=2:00, respectively. Both apolar cells are at an outer position. (t=5:30) After this time point, apolar cells are gradually internalized. (t=7:30) The edges of surrounding polar cells are moving closer (yellow arrowheads). (t=8:45) The surface of apolar cells is completely covered by polar cells. See supplementary material Movie 1.

Fig. S2G, only one apolar cell repolarized out of 101 asymmetric divisions observed; see also Fig. 3). Therefore, we concluded that the number of polar/apolar cells in the 16-cell embryo indicates the number of asymmetric divisions during the 8-16 cell division. Based on this, we estimated the frequency of asymmetric division in flushed and cultured CD1 embryos as 78% and 70% of 8-cell blastomeres (6.2 cells and 5.6 cells in the 8-cell embryo), respectively.

Next, we analyzed the outer/inner cell position of all 16 cells in the same set of embryos. We scored cell position based on any presence of a surface-exposed area based on F-actin staining. Interestingly, the number of inner cells was much smaller than the number of apolar cells. Freshly flushed CD1 embryos had an average number of 2.7±0.33 inner cells/embryo, spread from 0 to 5 (Fig. 2A). In cultured embryos, the average number was 1.1±0.15 cells/embryo spread from 0 to 3 (Fig. 2B). These numbers were consistent with the result of Dietrich and Hiiragi (2007) (Table 1). Confocal images clearly showed that the embryo surface was not fully encompassed by apical domains at the 16-cell stage, and that many apolar cells had surface exposure and were positioned outside (Fig. 1B,C).

To examine the fate of outer apolar cells, we performed live imaging analysis with Gap43-GFP (Moriyoshi et al., 1996) and Ezrin-RFP to visualize cell shape and apical domains, respectively. As shown in Fig. 2E (supplementary material Fig. S2G, Movie 1), apolar outer cells were gradually internalized by surrounding polar cells. This suggests that the outer/inner configuration of polar/apolar cells is not a simple result of orientation of divisions with respect to the embryo surface but is an active cell-sorting process.

Apolar daughters placed outside after asymmetric divisions have higher phospho-YAP in the cytoplasm

Regulation of the Hippo signaling cascade is important for formation of the TE and ICM lineages (Cockburn et al., 2013; Hirate et al., 2013; Leung and Zernicka-Goetz, 2013; Nishioka et al., 2009; Sasaki, 2010). We confirmed that in late morula and blastocyst embryos, outer polar cells had nuclear YAP and low cytoplasmic phospho-YAP, whereas inner apolar cells had no

Development (2014) 141, 2813-2824 doi:10.1242/dev.107276

Table 1. The number of outer/inner cells in 16-cell stage mouse embryos found in this and previous studies

Ratios of outer/inner cells at the 16-cell stage	Mouse strain	Methods	Reference
Transient labeling and dissociation			
10.8 outer/5.2 inner (9:7-14:2)	MFI	Rhodamine-ConA. Dissociation	Fleming (1987)
9.4 outer/6.6 inner (8:8-11:5)	F1 (C57/Bl6xCBA)	Microsphere labeling. Dissociation	Suwinska et al. (2008)
Live imaging and nuclear position			
13.2/2.8 (11:5-15:1)	F1 (C57/Bl6xCBA)	Live imaging (H2B-GFP mouse line). Nuclear position	Morris et al. (2010)
11.2/4.8	CD1	Live imaging. Single 8-cell tracing with nuclear and membrane markers	Yamanaka et al. (2010)
11.6 outer/3.4 intermediate/1 inner	CD1	Live imaging (H2B-GFP mouse line). Nuclear position	McDole et al. (2011)
F-actin staining and confocal imaging			
1 or 0 inside cells	F1 (C57/Bl6xC3H)	F-actin and nuclear staining	Dietrich and Hiiragi (2007)
F-actin, p-ERM staining and confocal imaging			
9.8 polar/6.2 apolar (8:8-14:2) 13.3 outer/2.7 inner (11:5-16:0)	CD1 flushed	p-ERM, F-actin and nuclear staining	This study
10.4 polar/5.6 apolar (8:8-14:2) 14.9 outer/1.1 inner (13:3-16:0)	CD1 cultured		
10.5 polar/5.5 apolar (8:8-14:2) 12.6 outer/3.4 inner (10:6-16:0)	C57/Bl6 flushed		
11.7 polar/4.3 apolar (8:8-15:1) 14.7 outer/1.3 inner (13:3-16:0)	C57/Bl6 cultured		

nuclear YAP and high cytoplasmic phospho-YAP (supplementary material Fig. S3). A difference in YAP localization and phosphorylation was observed as early as the 16-cell stage, but was not tightly correlated with the outer/inner positioning of the blastomeres (Fig. 3C,D; Fig. 4A). Although all polar cells were in an outer position and most had low cytoplasmic p-YAP, a few exceptional polar cells (Fig. 3B; 2-3% and 9-10% of the 16 cells in CD1 and B6 embryos, respectively) had high cytoplasmic p-YAP (Fig. 3C). Interestingly, these cells had relatively small apical domains and their nuclei were positioned further inward than in other polar cells (Fig. 3A,E). Smaller apical domains suggested that this minority of cells could be repolarizing apolar cells, because in the one case of repolarization of an apolar cell caught during live imaging analyses, the small apical domain expanded over time (Fig. 3F). Conversely, all inner apolar cells (Fig. 3B; 43% and 19% of total apolar cells in flushed and cultured CD1 embryos, respectively) had high cytoplasmic p-YAP, as expected. The majority of outer apolar cells also had high cytoplasmic p-YAP (53% and 63% of total apolar cells, respectively; Fig. 3B). The remaining outer apolar cells had low cytoplasmic p-YAP (Fig. 3D) and, interestingly, their nuclei were positioned more outward than in other apolar cells (Fig. 3A). Although we observed an interesting trend in nuclear position of the various categories of 16-cell blastomeres (Fig. 3A), we found that it is unreliable to use nuclear position as an indicator of polar/apolar or outer/inner designations, because the distribution of nuclear position in each category is largely overlapping.

Cell-cell contact is involved, but not essential to initiate differential p-YAP in polar/apolar cells

Next, we analyzed whether cell-cell contact affected the frequency of asymmetric divisions. We began by analyzing embryos cultured in Ca^{2+}-free media from the eight-cell stage to the 16-cell stage. We observed that blastomeres were rounded and non-adherent. Removal of the zona pellucida caused these cells to separate easily (Fig. 4B,B′, not shown). In these embryos, the number of polar cells ranged from 8 to 15, with an average of 10.6±0.39 cells (Fig. 4E). There was no significant difference between cultured CD1 embryos and embryos cultured in Ca^{2+}-free media (Mann-Whitney U-test, $P>0.05$). Next, we analyzed maternally deleted *Cdh1* mutant embryos, which lack adherens junctions (Boussadia et al., 2002). M (maternally deleted but zygotic heterozygous) $Cdh1^{+/-}$ embryos showed comparable morphology to wild-type embryos (not shown), suggesting that zygotically expressed E-cadherin had rescued the maternal phenotype by this stage. The number of polar cells ranged from 8 to 15 with an average of 10.0±0.42 cells (Fig. 4D). MZ (maternally and zygotic deleted) $Cdh1^{-/-}$ embryos showed a similar morphology to embryos cultured in Ca^{2+}-free media but to a lesser extent (Fig. 4C,C′). Residual cell-cell contact is likely regulated by other cell-adhesion molecules (Stephenson et al., 2010). The number of polar cells in MZ $Cdh1^{-/-}$ embryos ranged from 9 to 13 with an average of 11.1±0.31 polar cells, showing a distribution that appeared shifted to higher polar cell numbers (Fig. 4D). Accordingly, there was a significant difference in the distribution patterns of M $Cdh1^{+/-}$ and MZ $Cdh1^{-/-}$ embryo groups (Mann-Whitney U-test, $P<0.05$). From these data, we conclude that minimizing cell-cell adhesion in Ca^{2+}-free media after the 8-cell stage does not affect the frequency of asymmetric divisions during the 8-16 cell division. However, removing E-cadherin decreases the frequency of asymmetric divisions, suggesting that E-cadherin has a Ca^{2+}-independent function in the early embryo.

Next, we examined whether cell-cell contact and mouse strain differences affect p-YAP regulation. We analyzed pooled data from 14- to 18-cell embryos and found that more than 95% of polar cells in freshly flushed, cultured or Ca^{2+}-free cultured CD1 embryos had low cytoplasmic p-YAP (Fig. 4F). However, we observed a slight increase in the number of high p-YAP polar cells in B6, M $Cdh1^{+/-}$ and MZ $Cdh1^{-/-}$ embryos (14%, 12% and 10%, respectively) (Fig. 4C). This suggests that lack of cell-cell contact in Ca^{2+}-free media does not affect p-YAP regulation in polar cells, whereas lack of E-cadherin has a slight effect. However, we observed a much greater effect of cell-cell contact loss on p-YAP regulation in apolar cells (Fig. 4G). In flushed CD1 embryos, only 5% of apolar cells had low p-YAP in the cytoplasm. This increased up to 23% in cultured CD1 embryos. In CD1 embryos cultured in Ca^{2+}-free media, 62% of apolar cells had low p-YAP, although 38% of them still had high p-YAP without cell-cell contact (Fig. 4G). In M $Cdh1^{+/-}$ and MZ $Cdh1^{-/-}$ embryos, 45% and 54% of apolar cells had low p-YAP, respectively. These data suggest that E-cadherin-dependent cell-cell contact is important for YAP regulation,

Development (2014) 141, 2813-2824 doi:10.1242/dev.107276

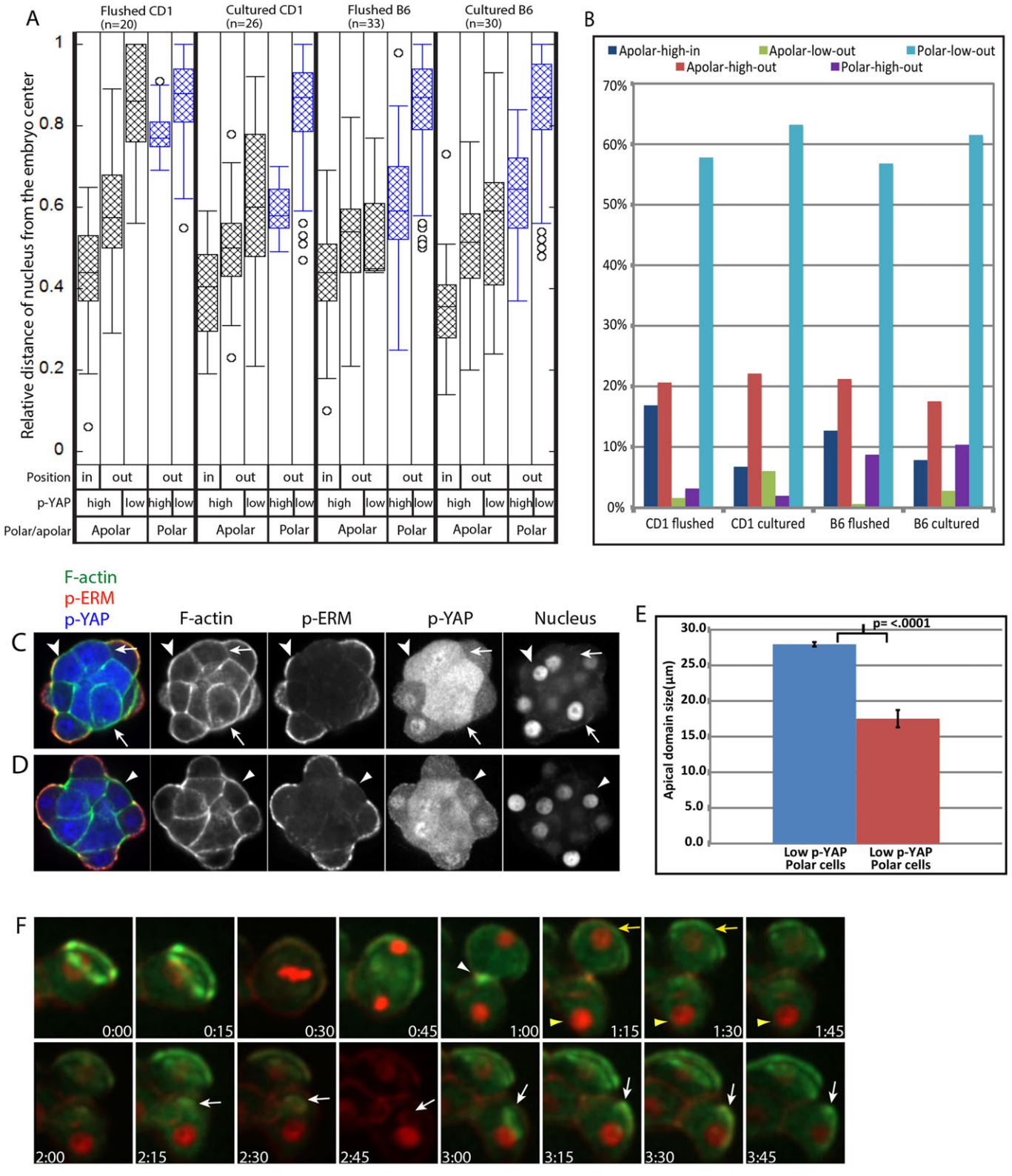

Fig. 3. Relationships between cell polarity, cell and nuclear position, and the state of YAP phosphorylation. (A) Flushed CD1 (*n*=20), cultured CD1 (*n*=26), flushed B6 (*n*=33) and cultured B6 (*n*=30) 16-cell embryos are compared. Blastomeres were divided into five categories based on cell polarity, cell position and the state of YAP phosphorylation. Nuclear positions are shown. (B) The proportion of 16-cell blastomeres in each category. (C) Embryo with an outer polar cell with high cytoplasmic p-YAP (arrowheads); outer apolar cells with high p-YAP (arrows). (D) Embryo with an outer apolar cell with low cytoplasmic p-YAP (arrowheads). (E) Polar cells with high p-YAP have significantly smaller apical domains than polar cells with low p-YAP. (F) Time-lapse images of a repolarizing apolar blastomere. An embryo labeled with Ezrin-GFP, membrane-RFP and H2b-RFP. Projected images. (t=0:00) One frame before entering mitosis. An Ezrin-enriched apical domain is visible. (t=0:15) Prophase. (t=0:30) Metaphase. (t=0:45) Telophase. (t=1:00) Cytokinesis. Contractile ring (white arrowhead). (t=1:15) Polar (yellow arrows) and apolar (yellow arrowheads) daughter cells. (t=2:15) A small Ezrin-enriched domain (arrow). (t=2:30-3:45) The Ezrin-enriched apical domain expands (arrows) (at t=2:45, the green Ezrin-GFP signal is missing due to an image acquisition error).

Development (2014) 141, 2813-2824 doi:10.1242/dev.107276

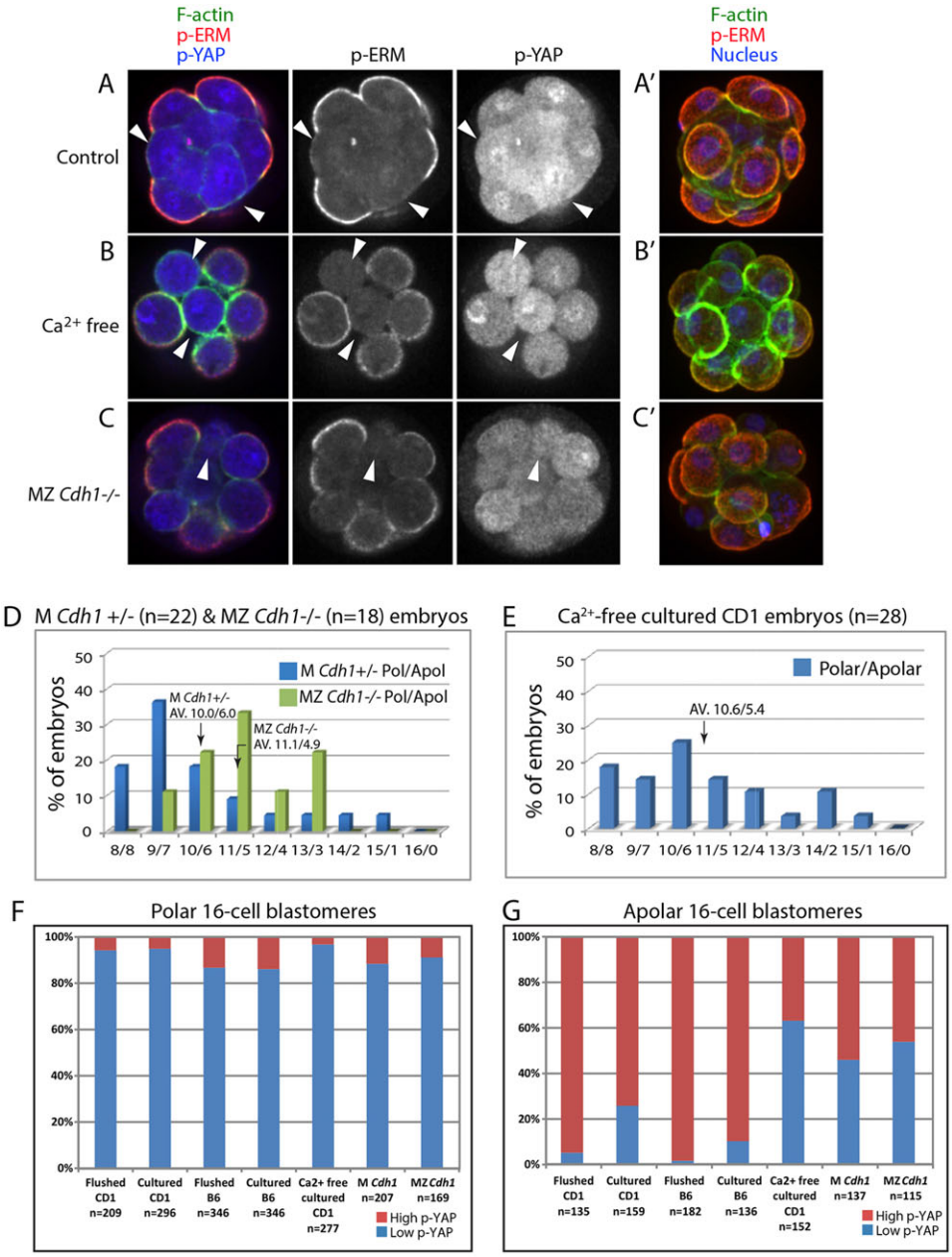

Fig. 4. Cell-cell contact is involved but not essential to initiate YAP phosphorylation in apolar cells. (A-C′) Upregulation of YAP phosphorylation was not restricted to inner cells. Many apolar cells exposed at embryo surface had high p-YAP staining in cytoplasm (arrowheads). (A,A′) Control embryo. (B,B′) Embryo cultured in Ca^{2+}-free KSOM from the 8-cell stage. Zona pellucida-constrained blastomeres touch, but do not adhere. (C,C′) MZ *Cdh1*$^{-/-}$ embryo, with occasional residual cell-cell contacts. (D,E) The number of polar/apolar and outer/inner cells at the 16-cell stage. (D) Cultured M *Cdh1*$^{+/-}$ (*n*=22) and MZ *Cdh1*$^{-/-}$ (*n*=18) 16-cell embryos. A significant difference was observed between M *Cdh1*$^{+/-}$ (*n*=22) and MZ *Cdh1*$^{-/-}$ (*n*=18) 16-cell embryos. (E) CD1 embryos cultured in Ca^{2+}-free conditions (*n*=28). The average numbers of polar/apolar cells and outer/inner cells are shown in each graph. (F) Frequency of high and low p-YAP in polar 16-cell blastomeres analyzed in embryos from 15-cell (i.e. one 8-cell blastomere and fourteen 16-cell blastomeres) to 18-cell (i.e. fourteen 16-cell blastomeres and four 32-cell blastomeres) stages. (G) Frequency of high and low p-YAP in apolar 16-cell blastomeres analyzed in embryos from 15-cell to 18-cell stages.

although it is not absolutely necessary, as some polar/apolar cells can still correctly regulate p-YAP localization.

Polar cells envelop apolar cells after the 8-16 cell division

Our time-lapse analyses showed that a cell internalization process establishes the outer/inner configuration of polar/apolar cells in intact embryos (Fig. 2E; supplementary material Movie 1). This process is also observed in isolated 8-cell blastomeres, which divide either symmetrically or asymmetrically during the 8-16 cell division to develop trophoblast vesicles and mini-blastocysts (Dietrich and Hiiragi, 2007; Johnson and Ziomek, 1983; Lorthongpanich et al., 2012).

To visualize this dynamic process, we performed live imaging analysis of isolated 8-cell blastomeres forming 2/16-cell couplets (Fig. 5; supplementary material Fig. S4 and Movie 2) and measured several physical parameters (Fig. 5F). When an isolated 8-cell blastomere divided symmetrically (Fig. 5A), the two daughter cells quickly established cell-cell contact and maximized the length of this contact (Fig. 5C). They maintained their opposed position with a flat contact boundary until the next division. Immunostaining confirmed that these couplets consisted of two polar cells (see Fig. 7C). By contrast, when an isolated 8-cell blastomere divided asymmetrically (Fig. 5B), the polar daughter cell enveloped the apolar daughter cell. Soon after the division, the two daughter cells quickly established a flat cell-cell contact (Fig. 5D, phase I), similar to the daughter cells after a symmetrical division. However, this flat cell-cell contact rapidly curved to a maximum curvature, i.e. the size of a spherical-shaped 16-cell blastomere (Fig. 5D, phase II). During curvature formation, the length of cell-cell contact was only slightly increased. After the maximum curvature was reached, the length of cell-cell contact started increasing as the enveloping process was initiated (Fig. 5D, phase III). Although there was variability in the speed of envelopment, the sequence of enveloping events appeared to be conserved (Fig. 5E; supplementary material Fig. S4).

Development (2014) 141, 2813-2824 doi:10.1242/dev.107276

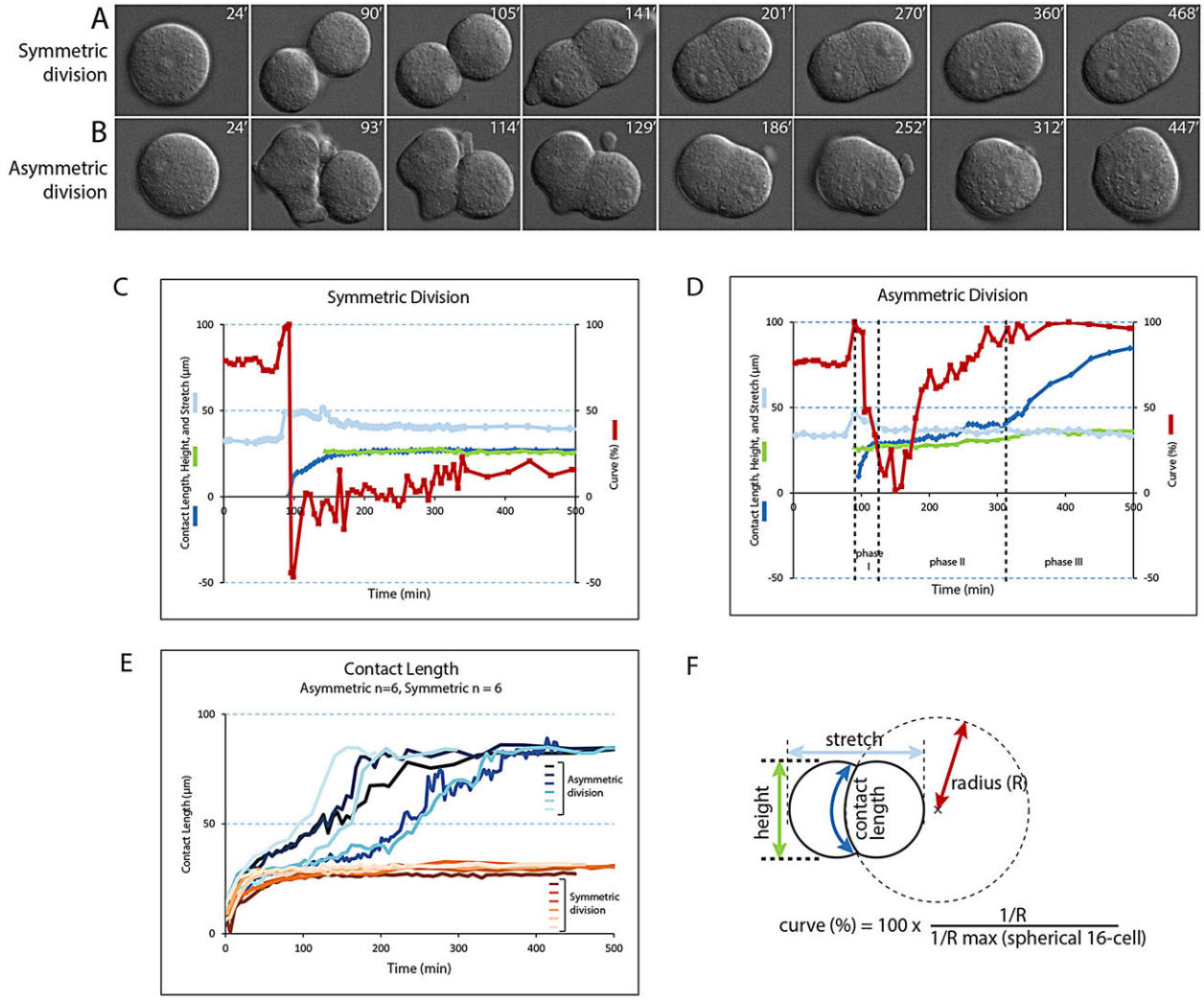

Fig. 5. Division dynamics in isolated 8-cell blastomeres. (A,B) Time-lapse images of isolated 8-cell blastomeres dividing symmetrically (A) or asymmetrically (B). Images were taken every 3 min. Time=0 is set at 30 min (10 frames) before nuclear envelope breakdown. (A) After completion of cytokinesis (t=90 min), two polar sister cells quickly establish cell-cell contact and are opposed. (B) After completion of cytokinesis (t=93 min), a polar (left) and an apolar (right) cell quickly establish cell-cell contact (by t=129 min). The cell-cell contact boundary curves toward the polar cell (t=129 to 252 min). The polar cell starts enveloping the apolar cell (t=312 to 447 min). (C,D) Quantification of four parameters of an isolated 8-cell blastomere dividing symmetrically (C) or asymmetrically (D). (D) Different phases are separated by dotted lines and represent a change in the slopes of the different graph series. (Phase I) Establishment of cell-cell contact where two daughter cells established a flat cell-cell contact. (Phase II) Curvature formation where cell-cell contact curved to a maximum curvature with minimum change in contact length. (Phase III) Envelopment where contact length started increasing as the enveloping process was initiated. (E) Variability in timing of envelopment in polar/apolar 2/16 couplets. (F) The parameters are: height (µm, green), stretch (µm, light blue), contact length (µm, blue) and curve (%, red). Curve is indicated as % of the maximum (defined as 1/radius (R) of a circle drawn to fit an enveloped 16-cell blastomere).

The difference in curvature formation observed at cell-cell contacts between polar cell couplets and polar/apolar cell couplets suggested that there was a difference in cortical contractility at the cell-cell contacts between polar and apolar cells soon after division. As the cortical actomyosin network regulates cellular cortical contractility (Amack and Manning, 2012; Salbreux et al., 2012), we examined the distribution of F-actin and phospho-myosin light chain II (p-MLCII). Although we did not observe any difference in the level of F-actin in polar/apolar cells, higher cortical localization of p-MLCII was observed in apolar cells (Fig. 6B,D,E), suggesting that the higher acto-myosin contractility in apolar cells generates the curvature at cell-cell contacts between polar and apolar cells. A p-MLCII difference was rarely observed in polar/polar couplets (Fig. 6A,C). This difference might initiate the envelopment of apolar cells by polar cells in order to set up outer/inner configuration (Krens and Heisenberg, 2011).

Phospho-YAP is differentially regulated soon after asymmetric division, but before establishment of an outer/inner configuration

We observed that many apolar cells in 16-cell embryos had an outer position and a high level of cytoplasmic p-YAP, similar to inner cells in later stage embryos. This suggested that the outer/inner configuration is not necessary to initiate differential p-YAP regulation. However, in intact embryos, it is not clear how long after 8-cell division polar/apolar 16-cell blastomeres establish differential p-YAP regulation. We therefore analyzed the timing of differential p-YAP regulation in 2/16 couplets undergoing asymmetric division.

First, we analyzed 2/16 couplets forming an outer/inner configuration for CDX2 expression, YAP localization and p-YAP regulation. We found that only outer polar cells had CDX2 and nuclear YAP localization (Fig. 7A,B), whereas inner cells had

Development (2014) 141, 2813-2824 doi:10.1242/dev.107276

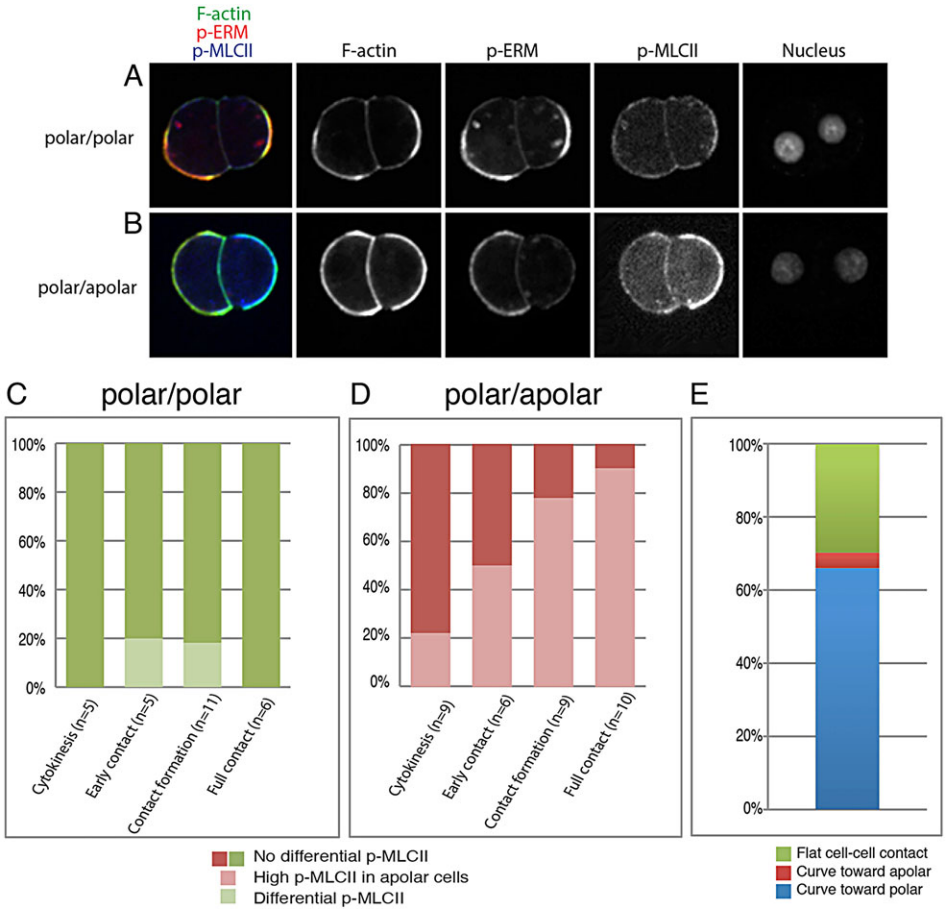

Fig. 6. MLCII phosphorylation is enriched at the cortex of apolar cells in 2/16 cell couplets. (A) Polar/polar 2/16 cell couplet. (B) Polar/apolar 2/16 cell couplet. p-MLCII is enriched at the cortex of an apolar cell in the polar/apolar 2/16 cell couplet. (C,D) Frequency of couplets showing asymmetric p-MLCII enrichment. (C) Polar/polar couplets. (D) Polar/apolar couplets. Cells with higher p-MLCII are always apolar cells. (E) Relationship between curving direction and cell polarity in polar/apolar couplets with high p-MLCII in apolar cells after contact formation.

cytoplasmic phosphorylated YAP, confirming that 2/16 couplets recapitulated the lineage specification process of intact embryos. Next, we analyzed 2/16 couplets within 2 h of division by visualizing the apical domain by the prominent ring pattern of F-actin enrichment (Fig. 7C,D). At this stage, both polar and apolar cells had an equal level of YAP nuclear localization. However, consistent with the results in intact embryos, apolar cells that were still unenveloped had higher cytoplasmic p-YAP (Fig. 7D). We further examined whether p-YAP was asymmetrically inherited during division. By the end of cytokinesis, there was no p-YAP difference in polar/apolar cells, whereas p-ERM apical localization was maintained during division (Fig. 7E). During cell-cell contact formation after cytokinesis (Phase I in Fig. 5D), 42% of polar/apolar couplets showed high p-YAP in apolar cells (Fig. 7H). By 2 hours after division, when couplets had established full contact (Fig. 7F), 90% of polar/apolar couplets showed high p-YAP in apolar cells (Fig. 7H). As expected, no increase of p-YAP was observed during this process in polar/polar couplets (Fig. 7G). This result suggests that upstream p-YAP regulators (or their activities) are asymmetrically inherited, rather than having asymmetric p-YAP distribution. Taken together, we conclude that polar/apolar cells have intrinsic differences that induce differential YAP regulation before establishing outer/inner positions in the embryo.

DISCUSSION

A long-standing goal in the field of mammalian development is to understand the mechanisms generating the first lineages derived from totipotent blastomeres. In the mouse embryo, the first two distinct populations arise after the 8-16 cell division. Asymmetrical divisions during the 8-16 cell division generate polar and apolar daughter cells by asymmetric inheritance of the apical domain. Polar cells take outer positions and apolar cells take inner positions in order to become TE and ICM in the blastocyst, respectively.

Several studies examined the number of outer/inner cells at the 16-cell stage using various methods. Classically, the embryo surface is transiently labeled with antibodies, lectins or small beads, and subsequently dissociated for cell counting (Fleming, 1987; Suwinska et al., 2008). These studies consistently identified five or six inner cells with a range from two to eight (Table 1). However, our study, as well as a previous study (Dietrich and Hiiragi, 2007), showed that only one or two cells are fully internalized in intact embryos at the 16-cell stage (Fig. 2). As it is known that endocytic activity is higher in TE and polarized blastomeres (Johnson et al., 1986), it is likely that the transient surface labeling methods selectively labeled polar cells rather than all outer cells. In other studies, nuclear position has been used to evaluate outer/inner cell positions during live imaging of mouse embryos carrying the H2B-GFP transgene (Morris et al., 2010; McDole et al., 2011). As we show in Fig. 3A, nuclear position alone is not a good indicator for either outer/inner cell position or polar/apolar cell polarity, although there is a trend in the distributions. We conclude from these studies and our current study that it is necessary to directly analyze cell polarity as well as cell position in intact embryos to understand the frequency of asymmetric divisions and the relationship between cell position and lineage specification.

What generates outer/inner cells? In *Drosophila* neuroblast asymmetric divisions (Prehoda, 2009), the orientation of division plays an important role in producing two distinct daughter cells with

Development (2014) 141, 2813-2824 doi:10.1242/dev.107276

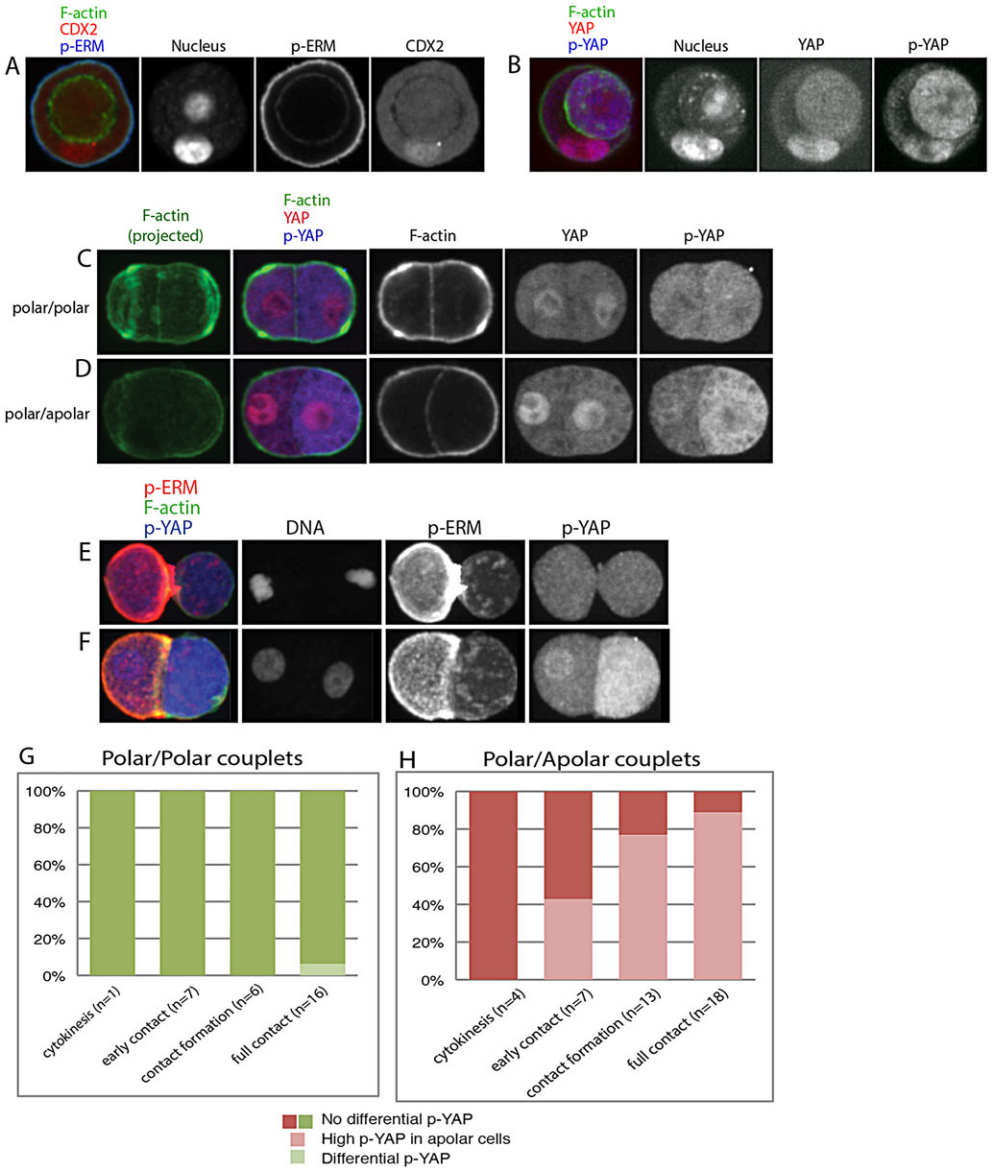

Fig. 7. Outer apolar cells show high p-YAP in cytoplasm before taking an inner position in 2/16 couplets. (A,B) 2/16 couplets forming the inner/outer configuration (5-6 h after division). (A) CDX2 is only expressed in the outer polar cell. (B) Nuclear YAP is only observed in the outer polar cell, whereas high cytoplasmic p-YAP is in the inner apolar cell. (C) A 2/16 couplet 2 h after symmetric division. (D) A 2/16 couplet 2 h after asymmetric division. The apolar cell (right) in the outer position has high cytoplasmic p-YAP. Cell-cell contact between the polar and apolar cell is curved toward the polar side, shown by F-actin staining. (E-H) High cytoplasmic p-YAP is quickly established during cell-cell contact formation after cytokinesis. (E) An asymmetrically dividing isolated 8-cell blastomere at cytokinesis. The apical domain marked by p-ERM staining was maintained during cytokinesis. No difference in the p-YAP level was observed between polar and apolar daughter cells. (F) A 2/16 couplet divides asymmetrically and establishes full contact. The apolar cell shows high cytoplasmic p-YAP. (G) Polar/polar 2/16 couplets show no sign of differential p-YAP levels. (H) Apolar cells quickly acquire high cytoplasmic p-YAP after cytokinesis, during establishment of cell-cell contact.

asymmetrically distributed lineage determinants in specifically allocated positions. However, in the mouse embryo, it has been shown that division orientation is not strictly regulated as parallel or perpendicular to the embryo surface. Indeed, many 8-cell blastomeres divide obliquely (Sutherland et al., 1990; Dard et al., 2009; Yamanaka et al., 2010; McDole et al., 2011) and both daughter cells are placed at an outer position soon after division regardless of the type of division. Here, we observed that many apolar cells are at an outer position at the 16-cell stage. Most of these cells will likely be internalized to take an inner position (Fig. 2E; supplementary material Movie 1; Yamanaka et al., 2010; McDole et al., 2011). We found two types of interesting (though minor) populations; outer apolar cells with low p-YAP (Fig. 3D) and outer polar cells with high p-YAP (Fig. 3C). Interestingly, the nuclei of both types of cells are positioned intermediately between other polar and apolar cells (Fig. 3A). McDole et al. also identified cells in an intermediate position between outer and inner cells at the 16-cell stage (McDole et al., 2011). Some of them divided asymmetrically in the 16-32 cell division, suggesting they were polar cells. Others divided symmetrically to generate two inner cells, suggesting they were apolar cells. These intermediate cells tended to have exposed outer surfaces but expressed low levels of CDX2. We speculate that polar cells with high p-YAP in our study represent the intermediate cells dividing asymmetrically in the McDole study. Interestingly, we found that these cells had a smaller sized apical domain, suggesting that p-YAP regulation is somehow dependent on the size of the apical domain. Our time-lapse movie analyses (Fig. 3F) suggests that polar cells with a small apical domain are in the process of repolarizing, although we could not fully exclude the possibility that a very small proportion of the apical domain is inherited, owing to the rare frequency of the event and the resolution of our time-lapse movies.

It is recognized that inner cells are generated not only during the 8-16 cell division, but also during the 16-32 cell division. It has recently been suggested that the difference in the timing of inner cell generation could create lineage bias in the ICM. Specifically, inner cells generated in the 1st round (the 8-16 cell division) are biased to become the epiblast (EPI) whereas those generated in the 2nd round (the 16-32 cell division) are biased to become the primitive endoderm (PE; Morris et al., 2010). However, we

Development (2014) 141, 2813-2824 doi:10.1242/dev.107276

did not observe such bias in a previous study (Yamanaka et al., 2010). Interestingly, in both studies, when an embryo had more inner cells at the 1st round, this bias was not observed (Morris, 2011; Yamanaka, 2011). Here, we show that the majority (75% in flushed, 60% in cultured) of CD1 embryos had high numbers of apolar cells (six to eight apolar cells) at the 16-cell stage, furthering the notion that cells generated in the 1st round are not biased.

We also observed a mouse strain effect on the number of apolar cells at the 16-cell stage. Only 37% of cultured B6 embryos had high numbers (6-8 cells) of apolar cells, which was significantly less than flushed and cultured CD1 embryos or flushed B6 embryos at the same stage (Fig. 2). B6 embryos appear susceptible to their environment, as seen in these *in vitro* cultures. Interestingly, both flushed and cultured B6 embryos had more high p-YAP polar cells compared with CD1 embryos (Fig. 3B, 9-10% in B6 versus 2-3% in CD1). This suggests that repolarization could be observed more frequently in B6 embryos. These results highlight that mouse strain should be considered when studying early mouse stages. Indeed, the use of different mouse strains in the above studies [B6/CBA F1 (Morris, 2011) and CD1 (Yamanaka, 2011)] could partly explain the different outcomes in the frequency of 1st round asymmetric divisions and lineage bias observed between the 1st and 2nd rounds.

Recently, higher expression of *Fgfr2* in inner cells generated in the 2nd round (Krupa et al., 2013; Morris et al., 2013) was reported, but it is not clear yet whether this difference is sufficient to create the PE/EPI ICM lineage bias. It will be interesting to examine whether the same mechanism (i.e. different expression levels of *Fgfr2* in individual inner cells) is used in PE/EPI specification in embryos with a high number of inner cells in the 1st round, which do not show apparent PE/EPI lineage bias (Morris, 2011; Morris et al., 2010; Yamanaka, 2011; Yamanaka et al., 2010).

Recent studies showed that angiomotin (Amot) is required in inner cells to activate Hippo signaling and phosphorylate YAP (Hirate et al., 2013; Leung and Zernicka-Goetz, 2013). Without Amot and Amotl2, a homolog with redundant functions to Amot, YAP phosphorylation is repressed and inner cells are specified as CDX2-expressing TE cells. Interestingly, lack of Amot and Amotl2 or modulation of other Hippo signaling molecules is sufficient to change YAP regulation but not to affect outer/inner configuration (Cockburn et al., 2013; Hirate et al., 2013; Leung and Zernicka-Goetz, 2013; Nishioka et al., 2009). This suggests that modulation of YAP signaling does not affect cell position and cell polarity. Our analysis of single isolated 8-cell blastomeres shows that p-YAP is differentially regulated in polar and apolar cells before setting up the outer/inner configuration in 2/16 cell couplets. This result suggests that inner positioning is not absolutely required to initiate Hippo signaling activation. In parallel, we observed a curved cell-cell boundary and increased cortical localization of p-MLCII in apolar cells preceding envelopment, suggesting that higher cortical tension in apolar cells occurs prior to inner cell positioning. These results indicate that polar and apolar cells have distinct intrinsic characteristics that may regulate differential Hippo signaling activation as well as establish the outer/inner configuration. There is evidence of a link between cell polarity and Hippo signaling in pre-implantation embryos, as Amot S176 phosphorylation is observed only in inner cells and regulated by Lats kinases (Hirate et al., 2013). It is suggested that the sequestration of Amot to the apical domain of outer cells may be a mechanism to block Hippo signaling activation. It will be interesting to examine whether polarity proteins directly interact with Hippo signaling components and how these interactions may affect establishment of the outer/inner configuration of blastomeres in the mouse embryo.

MATERIALS AND METHODS

Mice

Cdh1^{tm2Kem} mice (Boussadia et al, 2002) and Tg(Zp3-cre)93Knw (de Vries et al., 2000) were obtained from the Jackson Laboratory. C57BL/6 and CD1 mice were house bred or purchased from Harlan.

Embryo collection and culture

E0.5, E1.5 and E2.5 embryos were flushed from oviducts with FHM media (Millipore) and fixed or further cultured in KSOM media (Millipore). Drops of KSOM were covered with mineral oil in a humidified incubator at 37°C, 5% CO_2.

Isolation of single 8-cell blastomeres

After flushing, zona pellucidae were removed from 8-cell stage embryos (E2.5) with acid Tyrode's solution. Four zona-free embryos were exposed to Ca^{2+}-free KSOM at a time, for 15 min under mineral oil for de-compaction. Then, they were placed in FHM drops and dissociated with micro-needles (~30 µm openings) by gentle mouth pipetting. The isolated cells were transferred to micro-drop plates (one cell/drop), and incubated at 37°C, 5%CO_2. The blastomeres were inspected every 2 h under a dissecting microscope.

Immunostaining

Embryos were fixed in 4% formaldehyde (FA, Polyscience) in PBS for 10 min and stored in PBT (0.1% Tween 20 in PBS) at 4°C. For permeabilization, embryos were incubated at room temperature for 20 min in 0.2% Triton X-100 and 10% FBS in PBS and then blocked in 10% FBS in PBT for 1 h at room temperature. Embryos were treated in primary antibodies at 4°C, overnight in blocking solution. The embryos were washed in PBT for 1 h at room temperature and treated with secondary antibodies in PBT for 1 h at room temperature. After washing, the embryos were analyzed using a confocal microscope.

Primary antibodies used were: anti-YAP [1/100, sc101199; Santa Cruz Biotechnology (SCB)], anti-CDX2 (1/10, ab86949; Abcam), anti-phospho-ERM [1/500, #3149P; Cell Signaling Technology (CST)], anti-YAP/TAZ (1/100, #8418; CST), anti-P-MLCII (1/200, #3671P; CST), anti-P-YAP (1/100, #4911S; CST), anti-PARD6B (1/1000, sc67393; SCB), anti-uvomorulin (E-cadherin; 1/1000, U3254; Sigma). Secondary antibodies conjugated with Dylight or Alexafluor were purchased from Jackson ImmunoResearch and Molecular Probes; 1/400). A Zenon Alexa Fluor Labeling Kit (Molecular Probes, 546 goat anti-rabbit) was used for double rabbit primary antibody staining. For nuclear staining, Draq5 (BioStatus) or POPO-1 Iodide (Invitrogen) was used.

Image analysis

Confocal images and time-lapse movies were processed using the Volocity, Imaris 7.7 and Fiji-win32 software. Cell counting was performed using Imaris. The Surpass, Spots function of Imaris was used to identify nuclei. Nuclear diameter was estimated to be ~9 µm. We used true background subtraction and intensity threshholding for each channel with a Quality filter (the intensity at the center of the spot in the channel the spot was detected). Nuclear position was determined using Imaris spot function (x, y and z). The embryo center was identified as the center of all nuclear positions. Distance of each nucleus from the center was calculated and normalized to the maximum nuclear position in the embryo.

P-YAP signal was measured using the Imaris volume function where the average signal in the blastomere (excluding the nucleus) was determined for each polar and apolar blastomere. P-YAP was significantly higher in apolar blastomeres with an average of 3400±880 whereas in polar blastomeres it was 2000±380. ANOVA independent sample analysis was used for the statistical analysis and the *P*-value between polar and apolar cells was found

Development (2014) 141, 2813-2824 doi:10.1242/dev.107276

to be <0.01. Cortical P-MLCII signal was qualitatively scored by eye. All scoring were performed blindly without knowing polarity information.

Image analysis of 16-cell couplets

For live imaging of isolated blastomeres, a Zeiss Axio-observer with an environmental chamber was used with Axiovision software. A 20× objective (dry NA=0.8) was used. Three Z-images/time points were taken every 3 min. For image analysis, time=0 was chosen to be 30 min (10 frames) before nuclear membrane breakdown. Four physical parameters of 2/16-cell couplets were measured: contact length (µm), height (µm), stretch (µm) and curve (%) (see Fig. 5F). The curve was measured as the inverse relationship with the radius (1/R) and is presented at each curve value as % of the maximum value. We defined 100% (the maximum value) as the perfect spherical shape of a 16-cell blastomere (i.e. in 2D images, a circle drawn over a fully enveloped 16-cell blastomere). All measurements were performed with the Fiji software.

mRNA microinjection of fluorescent reporters

In vitro mRNA transcription was performed following the manufacturer's protocol (Ambion, SP6 message machine). Synthesized mRNAs were dissolved in water at 500-2000 ng/ml and injected into early blastomeres at the 2-, 4- and 8-cell stages. As previously described (Yamanaka et al., 2010), microinjection was performed using an Eppendorf Femtojet and WPI cyto721 electrometer for the tickler circuit. Success rates of injection were higher than 90%. Fluorescent reporters used were Ezrin-GFP/RFP (Batchelor et al., 2004), GAP43-GFP (Moriyoshi et al., 1996), membrane-RFP and H2b-RFP (Megason and Fraser, 2003).

Live imaging analysis of intact embryos

Two microscopes were used: (1) A Zeiss Axio observer equipped with an Apotome2, 20× objective (Zeiss Plan Apo ×20 NA=0.8), a Zeiss AxioCam MRm CCD camera and an environmental chamber (the medium grid was used for Apotome2 optical sections); (2) a Nikon swept field confocal (SFC) equipped with a 20× objective (Nikon Plan Apo ×20 NA=0.75), Andor iXon3 EM-CCD camera and an environmental chamber. Both 488 and 561 nm laser lines (Agilent MLC400) and 35 or 70 slit mode aperture were used. For both microscope set-ups, images were taken every 15 min, 8-10 Z-sections/time point and 5-10 µm section intervals. 3D projected images were generated using Imaris 7.7, Nikon NIS Elements AR 4.20.01 or Zeiss ZEN 2012. Maximum projection was used and smoothing was applied when necessary.

Acknowledgements

We thank the Goodman Cancer Research Centre Transgenic Facility for their help in preparation of timed pregnant females. We also thank the McGill CIAN imaging facility.

Competing interests

The authors declare no competing financial interests.

Author contributions

S.A. and Y.Y. conceived, designed and performed the experiments. S.A. and S.B. (Fig. 5 and supplementary material Fig. S4) analyzed the data. N.H.-Y. helped with genotyping and colony maintenance. S.A., D.K. and Y.Y. wrote and edited the paper.

Funding

This work was supported by Canada Foundation for Innovation [LOI25576] and Canadian Institutes of Health Research [MOP111197 and MOP107518].

Supplementary material

Supplementary material available online at
http://dev.biologists.org/lookup/suppl/doi:10.1242/dev.107276/-/DC1

References

Amack, J. D. and Manning, M. L. (2012). Knowing the boundaries: extending the differential adhesion hypothesis in embryonic cell sorting. *Science* **338**, 212-215.

Batchelor, C. L., Woodward, A. M. and Crouch, D. H. (2004). Nuclear ERM (ezrin, radixin, moesin) proteins: regulation by cell density and nuclear import. *Exp. Cell Res.* **296**, 208-222.

Berryman, M., Franck, Z. and Bretscher, A. (1993). Ezrin is concentrated in the apical microvilli of a wide variety of epithelial cells whereas moesin is found primarily in endothelial cells. *J. Cell Sci.* **105**, 1025-1043.

Blij, S., Frum, T., Akyol, A., Fearon, E. and Ralston, A. (2012). Maternal Cdx2 is dispensable for mouse development. *Development* **139**, 3969-3972.

Boussadia, O., Kutsch, S., Hierholzer, A., Delmas, V. and Kemler, R. (2002). E-cadherin is a survival factor for the lactating mouse mammary gland. *Mech. Dev.* **115**, 53-62.

Cockburn, K., Biechele, S., Garner, J. and Rossant, J. (2013). The Hippo pathway member Nf2 is required for inner cell mass specification. *Curr. Biol.* **23**, 1195-1201.

Dard, N., Louvet, S., Santa-Maria, A., Aghion, J., Martin, M., Mangeat, P. and Maro, B. (2001). In vivo functional analysis of ezrin during mouse blastocyst formation. *Dev. Biol.* **233**, 161-173.

Dard, N., Louvet-Vallée, S. and Maro, B. (2009). Orientation of mitotic spindles during the 8- to 16-cell stage transition in mouse embryos. *PLoS One* **4**, e8171.

de Vries, W. N., Binns, L. T., Fancher, K. S., Dean, J., Moore, R., Kemler, R. and Knowles, B. B. (2000). Expression of Cre recombinase in mouse oocytes: a means to study maternal effect genes. *Genesis* **26**, 110-112.

Dietrich, J.-E. and Hiiragi, T. (2007). Stochastic patterning in the mouse pre-implantation embryo. *Development* **134**, 4219-4231.

Fehon, R. G., McClatchey, A. I. and Bretscher, A. (2010). Organizing the cell cortex: the role of ERM proteins. *Nat. Rev. Mol. Cell Biol.* **11**, 276-287.

Fleming, T. P. (1987). A quantitative analysis of cell allocation to trophectoderm and inner cell mass in the mouse blastocyst. *Dev. Biol.* **119**, 520-531.

Hirate, Y., Hirahara, S., Inoue, K.-i., Suzuki, A., Alarcon, V. B., Akimoto, K., Hirai, T., Hara, T., Adachi, M., Chida, K. et al. (2013). Polarity-dependent distribution of angiomotin localizes Hippo signaling in preimplantation embryos. *Curr. Biol.* **23**, 1181-1194.

Hogan, B. and Tilly, R. (1978). In vitro development of inner cell masses isolated immunosurgically from mouse blastocysts. I. Inner cell masses from 3.5-day p.c. blastocysts incubated for 24 h before immunosurgery. *J. Embryol. Exp. Morphol.* **45**, 93-105.

Johnson, M. H. and Ziomek, C. A. (1981). The foundation of two distinct cell lineages within the mouse morula. *Cell* **24**, 71-80.

Johnson, M. H. and Ziomek, C. A. (1983). Cell interactions influence the fate of mouse blastomeres undergoing the transition from the 16- to the 32-cell stage. *Dev. Biol.* **95**, 211-218.

Johnson, M. H., Chisholm, J. C., Fleming, T. P. and Houliston, E. (1986). A role for cytoplasmic determinants in the development of the mouse early embryo? *J. Embryol. Exp. Morphol.* **97** Suppl, 97-121.

Krens, S. F. and Heisenberg, C. P. (2011). Cell sorting in development. *Curr. Top. Dev. Biol.* **95**, 189-213.

Krupa, M., Mazur, E., Szczepanska, K., Filimonow, K., Maleszewski, M. and Suwinska, A. (2013). Allocation of inner cells to epiblast vs primitive endoderm in the mouse embryo is biased but not determined by the round of asymmetric divisions (8–>16- and 16–>32-cells). *Dev. Biol.* **385**, 136-148.

Leung, C. Y. and Zernicka-Goetz, M. (2013). Angiomotin prevents pluripotent lineage differentiation in mouse embryos via Hippo pathway-dependent and -independent mechanisms. *Nat. Commun.* **4**, 2251.

Lorthongpanich, C., Doris, T. P. Y., Limviphuvadh, V., Knowles, B. B. and Solter, D. (2012). Developmental fate and lineage commitment of singled mouse blastomeres. *Development* **139**, 3722-3731.

Louvet, S., Aghion, J., Santa-Maria, A., Mangeat, P. and Maro, B. (1996). Ezrin becomes restricted to outer cells following asymmetrical division in the preimplantation mouse embryo. *Dev. Biol.* **177**, 568-579.

McDole, K., Xiong, Y., Iglesias, P. A. and Zheng, Y. (2011). Lineage mapping the pre-implantation mouse embryo by two-photon microscopy, new insights into the segregation of cell fates. *Dev. Biol.* **355**, 239-249.

Megason, S. G. and Fraser, S. E. (2003). Digitizing life at the level of the cell: high-performance laser-scanning microscopy and image analysis for in toto imaging of development. *Mech. Dev.* **120**, 1407-1420.

Moriyoshi, K., Richards, L. J., Akazawa, C., O'Leary, D. D. M. and Nakanishi, S. (1996). Labeling neural cells using adenoviral gene transfer of membrane-targeted GFP. *Neuron* **16**, 255-260.

Morris, S. A. (2011). Cell fate in the early mouse embryo: sorting out the influence of developmental history on lineage choice. *Reprod. Biomed. Online* **22**, 521-524.

Morris, S. A., Teo, R. T. Y., Li, H., Robson, P., Glover, D. M. and Zernicka-Goetz, M. (2010). Origin and formation of the first two distinct cell types of the inner cell mass in the mouse embryo. *Proc. Natl. Acad. Sci. U.S.A.* **107**, 6364-6369.

Morris, S. A., Graham, S. J. L., Jedrusik, A. and Zernicka-Goetz, M. (2013). The differential response to Fgf signalling in cells internalized at different times influences lineage segregation in preimplantation mouse embryos. *Open Biol.* **3**, 130104.

Nishioka, N., Inoue, K.-i., Adachi, K., Kiyonari, H., Ota, M., Ralston, A., Yabuta, N., Hirahara, S., Stephenson, R. O., Ogonuki, N. et al. (2009). The Hippo signaling pathway components Lats and Yap pattern Tead4 activity to distinguish mouse trophectoderm from inner cell mass. *Dev. Cell* **16**, 398-410.

Development (2014) 141, 2813-2824 doi:10.1242/dev.107276

Prehoda, K. E. (2009). Polarization of Drosophila neuroblasts during asymmetric division. *Cold Spring Harb. Perspect. Biol.* **1**, a001388.

Ralston, A. and Rossant, J. (2008). Cdx2 acts downstream of cell polarization to cell-autonomously promote trophectoderm fate in the early mouse embryo. *Dev. Biol.* **313**, 614-629.

Saiz, N. and Plusa, B. (2013). Early cell fate decisions in the mouse embryo. *Reproduction* **145**, R65-R80.

Salbreux, G., Charras, G. and Paluch, E. (2012). Actin cortex mechanics and cellular morphogenesis. *Trends Cell Biol.* **22**, 536-545.

Sasaki, H. (2010). Mechanisms of trophectoderm fate specification in preimplantation mouse development. *Dev. Growth Differ.* **52**, 263-273.

Spindle, A. I. (1978). Trophoblast regeneration by inner cell masses isolated from cultured mouse embryos. *J. Exp. Zool.* **203**, 483-489.

Stephenson, R. O., Yamanaka, Y. and Rossant, J. (2010). Disorganized epithelial polarity and excess trophectoderm cell fate in preimplantation embryos lacking E-cadherin. *Development* **137**, 3383-3391.

Strumpf, D., Mao, C.-A., Yamanaka, Y., Ralston, A., Chawengsaksophak, K., Beck, F. and Rossant, J. (2005). Cdx2 is required for correct cell fate specification and differentiation of trophectoderm in the mouse blastocyst. *Development* **132**, 2093-2102.

Sutherland, A. E., Speed, T. P. and Calarco, P. G. (1990). Inner cell allocation in the mouse morula: the role of oriented division during fourth cleavage. *Dev. Biol.* **137**, 13-25.

Suwińska, A., Czolowska, R., Ożdżeński, W. and Tarkowski, A. K. (2008). Blastomeres of the mouse embryo lose totipotency after the fifth cleavage division: expression of Cdx2 and Oct4 and developmental potential of inner and outer blastomeres of 16- and 32-cell embryos. *Dev. Biol.* **322**, 133-144.

Wu, G., Gentile, L., Fuchikami, T., Sutter, J., Psathaki, K., Esteves, T. C., Arauzo-Bravo, M. J., Ortmeier, C., Verberk, G., Abe, K. et al. (2010). Initiation of trophectoderm lineage specification in mouse embryos is independent of Cdx2. *Development* **137**, 4159-4169.

Yamanaka, Y. (2011). Response: cell fate in the early mouse embryo–sorting out the influence of developmental history on lineage choice. *Reprod. Biomed. Online* **22**, 525-527; discussion 528.

Yamanaka, Y., Ralston, A., Stephenson, R. O. and Rossant, J. (2006). Cell and molecular regulation of the mouse blastocyst. *Dev. Dyn.* **235**, 2301-2314.

Yamanaka, Y., Lanner, F. and Rossant, J. (2010). FGF signal-dependent segregation of primitive endoderm and epiblast in the mouse blastocyst. *Development* **137**, 715-724.

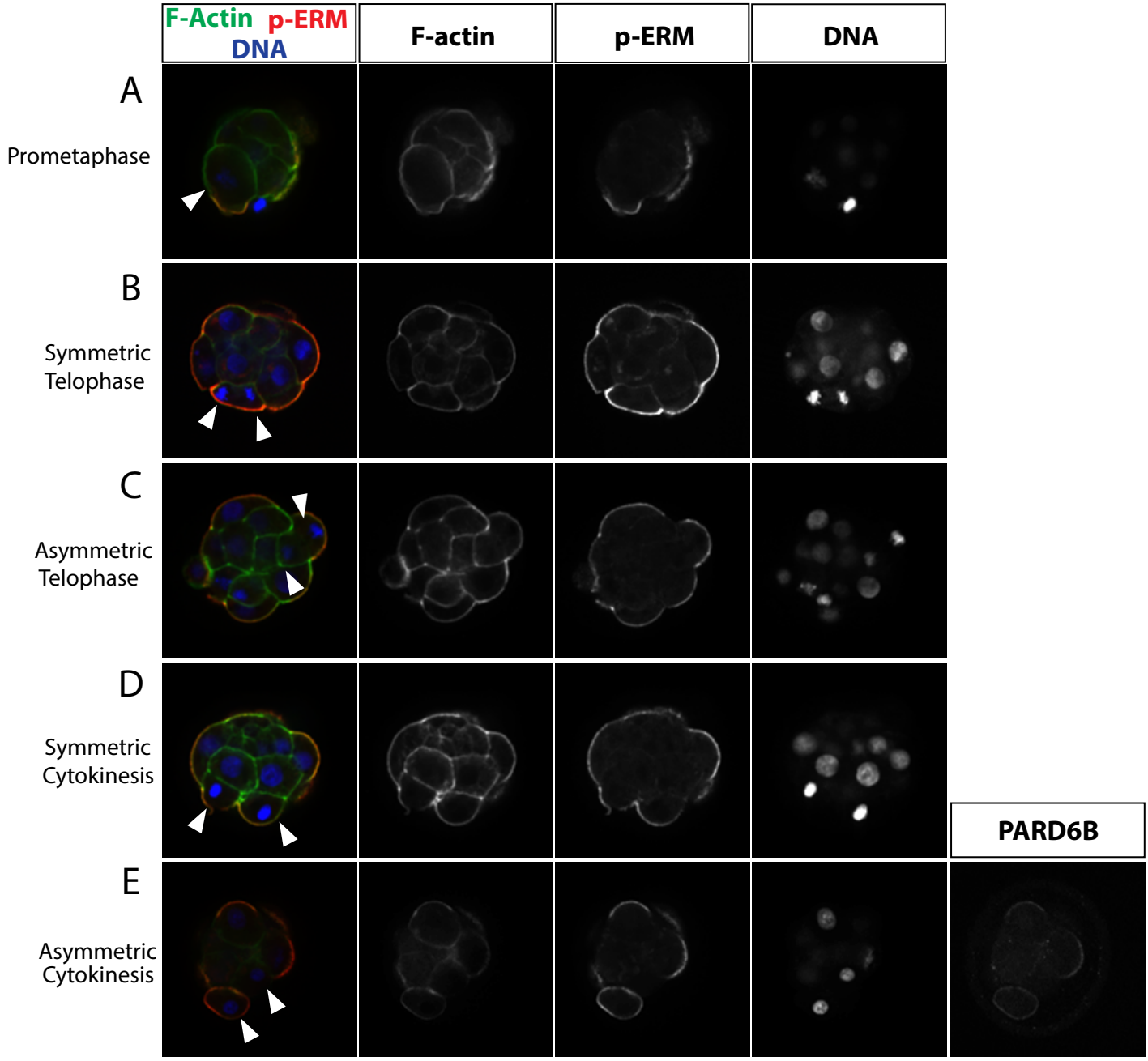

Supplementary Figure 1.
Apical domains are maintained during 8-16 cell divisions.
A. Prometaphase. B. Telophase of symmetric division. C. Telophase of asymmetric division. D. Cytokinesis of symmetric division. E. Cytokinesis of asymmetric division. p-ERM and PARD6B localization at the apical domain are maintained through the mitotic phase.

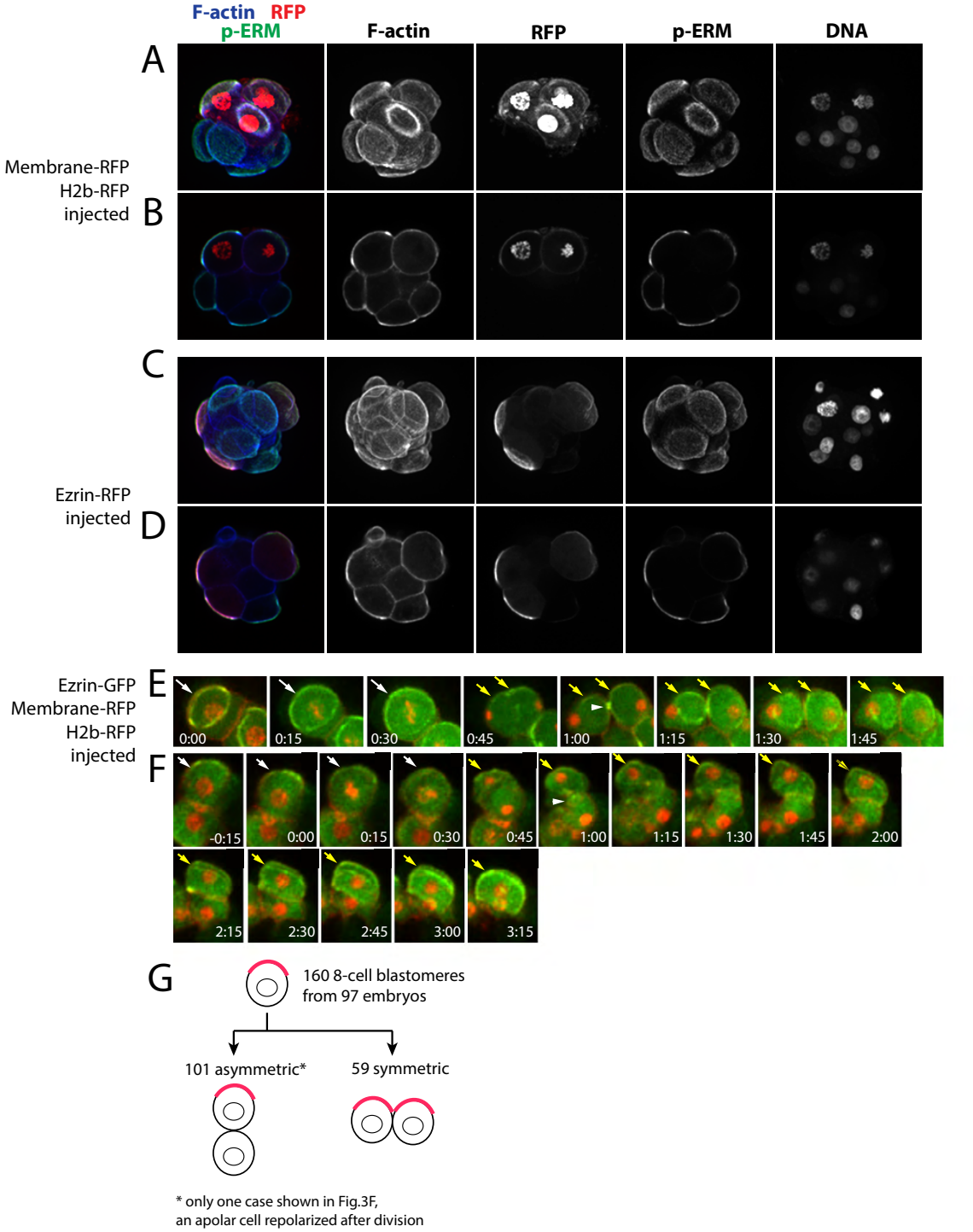

Supplementary Figure 2.
Fluorescent reporters, membrane-RFP and Ezrin GFP/RFP are enriched at the apical domain in progeny of mRNA injected blastomeres.
A and B. Membrane-RFP and histone H2b-RFP injected embryo. mRNAs of the reporters were injected into one of 2-cell blastomeres. A. Projected images. B. Optical section images. Membrane-RFP is enriched at the apical domain marked by F-actin and p-ERM staining. C and D. Ezrin-RFP injected embryo. C. Projected images. D. Optical section images. Ezrin-RFP enrichment co-localized with p-ERM staining. E and F. Time-lapse images of Ezrin-GFP, membrane-RFP and H2B-RFP injected embryos. Projected images. E. 8-cell blastomere dividing symmetrically. (t=0:00) One frame (15min) before entering mitosis. An apical domain is clearly visible (arrows). (t=0:30) Metaphase. (t=1:00) Cytokinesis. Contractile ring (arrowhead). (t=1:30) Two daughter polar 16-cells (yellow arrows). F. 8-cell blastomere dividing asymmetrically. (t=0:00) One frame before entering mitosis. Apical domain (arrows). (t=0:30) Prometaphase. (t=1:00) Cytokinesis. (t=1:30) One polar (yellow arrows) and one apolar daughter cell. (t=2:45) The apolar cell internalizes. Interestingly, Ezrin-GFP enrichment becomes less clear during cell division in live imaging, although it is still enriched in the fixed embryo shown in C and D. G. Schematic of division patterns of single 8-cell blastomeres. A total of 160 8-cell blastomeres from 97 embryos were observed. 101 blastomeres divided asymmetrically and 59 blastomeres divided symmetrically. Only one apolar cell repolarized after asymmetric division.

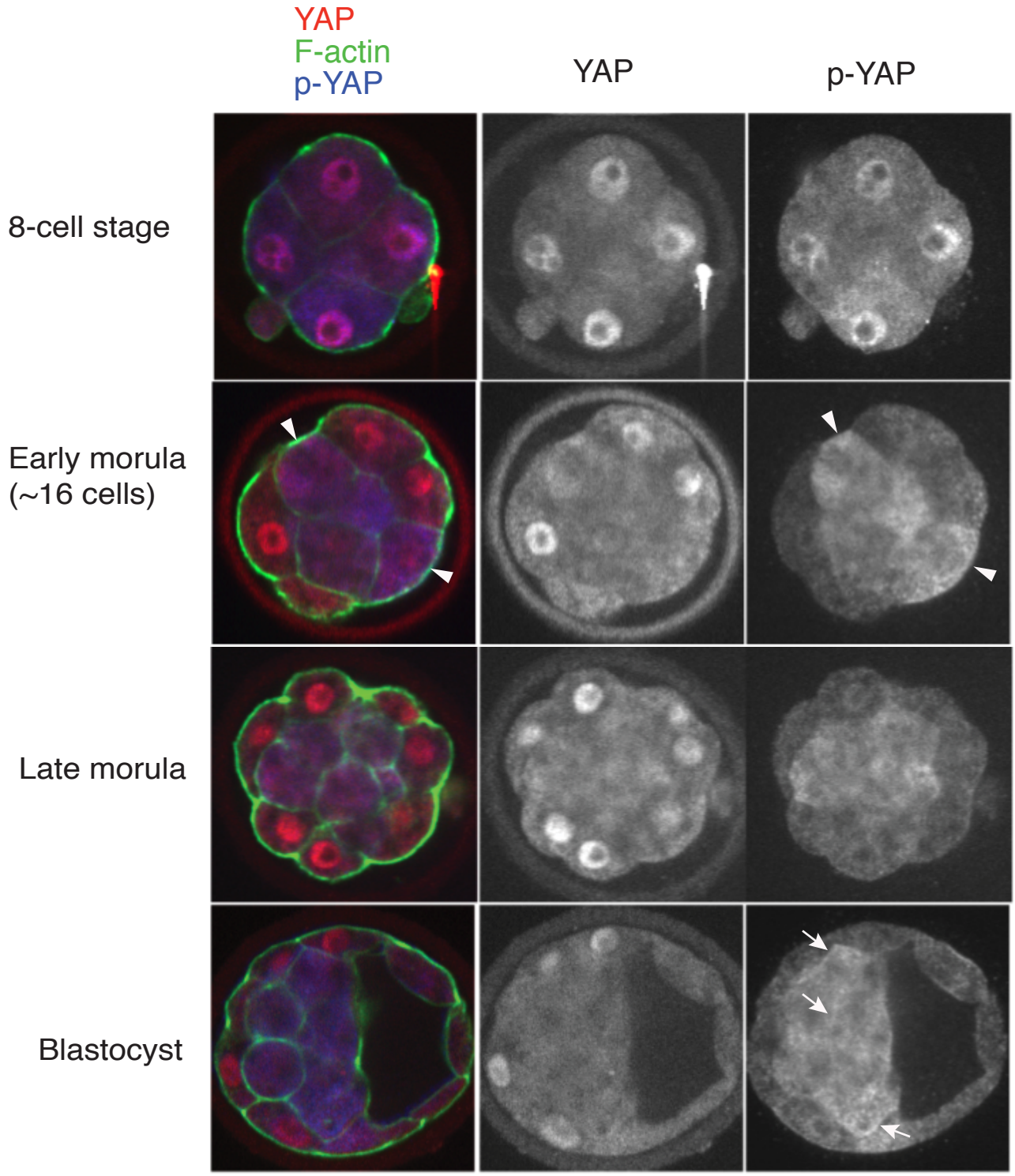

Supplementary Figure 3.
YAP and phosphorylated YAP (p-YAP) localization in preimplantation mouse embryos.

8-cell stage. YAP nuclear localization is observed in all blastomeres. At this stage, p-YAP is also localized in the nucleus.
Early morula stage (~16 cells). Polar cells show YAP nuclear localization with low levels of p-YAP in the nucleus and cytoplasm, while apolar cells show higher cytoplasmic p-YAP. No YAP nuclear localization in apolar cells. At this stage, some apolar cells are at outer positions (white arrowheads).
Late morula stage (~32 cells). Outer polar cells show YAP nuclear localization with low levels of pYAP, while apolar cells show higher cytoplasmic p-YAP. By this stage, all apolar cells are located at inner positions with high p-YAP in the cytoplasm.
Blastocyst stage. Outer TE cells show YAP nuclear localization while ICM cells show high p-YAP in the cytoplasm. Enrichment of p-YAP at cell membrane/cortex is observed (white arrows).

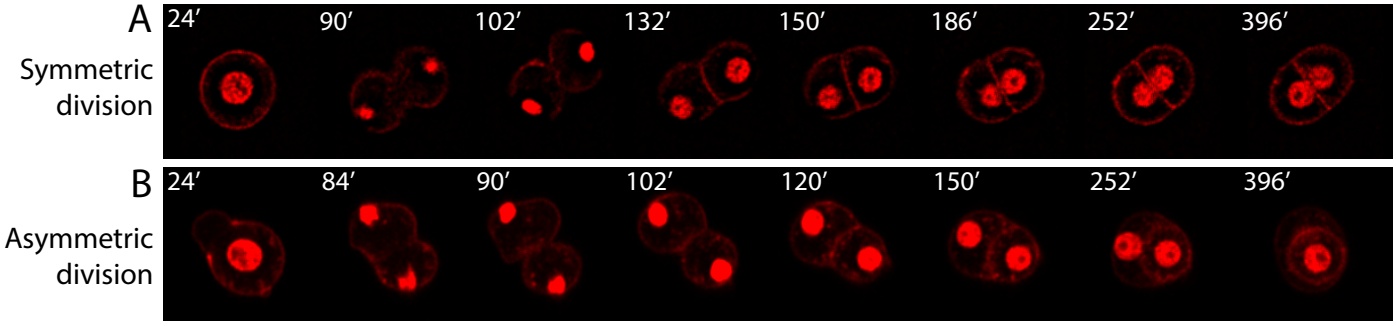

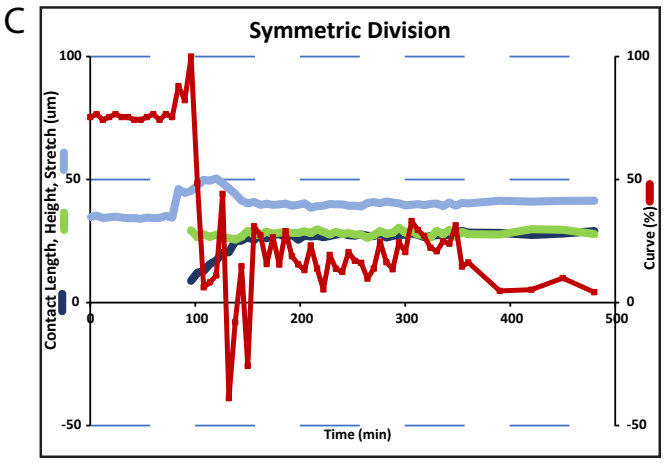

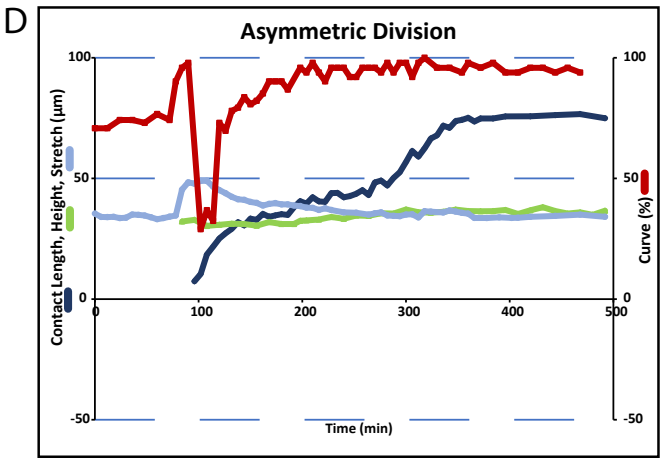

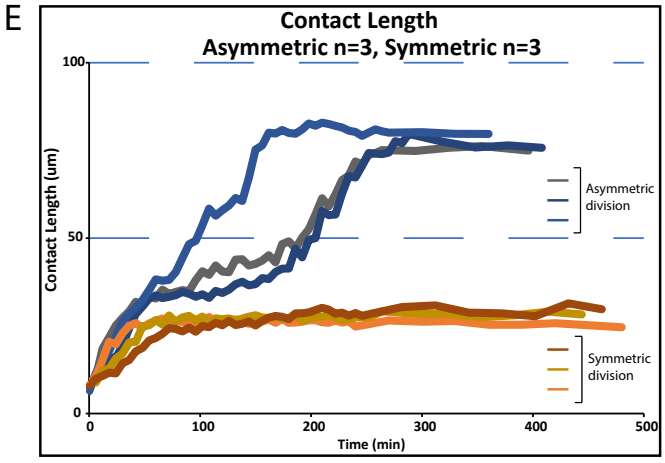

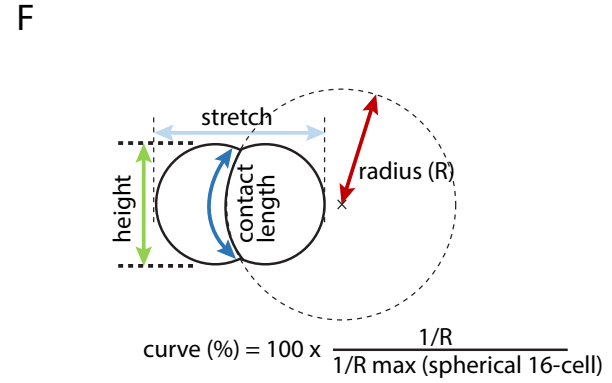

Supplementary figure 4.
Division dynamics in isolated 8-cell blastomeres injected with membrane-RFP and H2b-RFP mRNAs.
A, B. Time-lapse images of isolated 8-cell blastomeres dividing symmetrically (A) or asymmetrically (B). Images were taken every 3 minutes (min). Time= 0 is set at 30 min (10 frames) before nuclear envelope breakdown. A. After completion of cytokinesis (t=102 min), two polar sister cells quickly establish cell-cell contact and are opposed. B. After completion of cytokinesis (t=90 min), a polar (left) and an apolar (right) cell quickly establish cell-cell contact (by t=102 min). The cell-cell contact boundary curves toward the polar cell (t= 120 to 252 min). The polar cell starts enveloping the apolar cell (t= 253 to 396 min). C and D. Quantification of four parameters of membrane- and H2b-RFP mRNA-injected isolated 8-cell blastomere dividing symmetrically (C) or asymmetrically (D). E. Variability in timing of envelopment in polar/apolar 2/16 couplets. Basically, we observed the same cell dynamics observed in DIC images shown Figure 5. F. The parameters are: Height (µm, green), stretch (µm, light blue), contact length (µm, blue) and curve (%, red). Curve is indicated as % of the maximum (defined as 1/R of a circle drawn to fit an enveloped 16-cell blastomere).

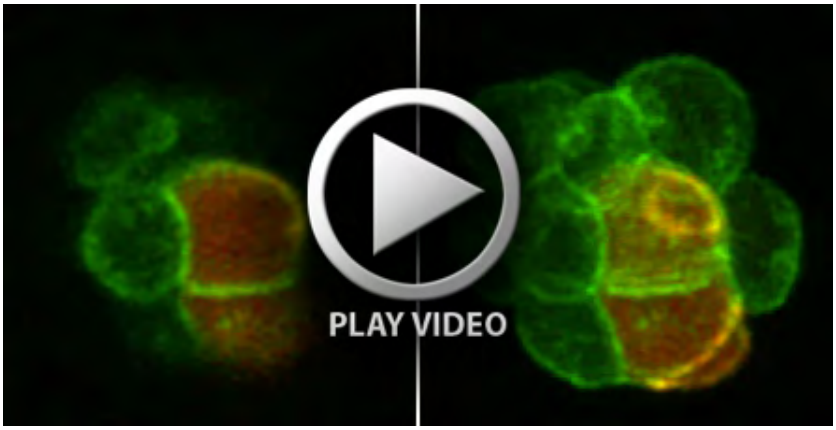

Supplementary movie 1.
Time-lapse movie showing the internalization process of apolar outer cells. The embryo is labeled with GAP-43 GFP for cell shape visualization and Ezrin-RFP for apical domain visualization. The left movie shows optical section images at Z=2 and the right movie shows projected images generated from 9 optical sections. 15 min/frame.

Supplementary movie 2.
Time-lapse movie showing divisions of isolated 8-cell blastomeres and subsequent 16-cell couplet formation. The left movie shows a blastomere dividing symmetrically and the right shows one dividing asymmetrically. Three Z-section images were collected. The middle section is shown. 3 min/frame.